Model for the Light-Harvesting Complex I (B875) of *Rhodobacter sphaeroides*

Xiche Hu and Klaus Schulten

Beckman Institute and Department of Physics, University of Illinois at Urbana-Champaign, Urbana, Illinois 61801 USA

ABSTRACT   The light-harvesting complex I (LH-I) of *Rhodobacter sphaeroides* has been modeled computationally as a hexadecamer of $\alpha\beta$-heterodimers, based on a close homology of the heterodimer to that of light-harvesting complex II (LH-II) of *Rhodospirillum molischianum*. The resulting LH-I structure yields an electron density projection map that is in agreement with an 8.5-Å resolution electron microscopic projection map for the highly homologous LH-I of *Rs. rubrum*. A complex of the modeled LH-I with the photosynthetic reaction center of the same species has been obtained by a constrained conformational search. This complex and the available structures of LH-II from *Rs. molischianum* and *Rhodopseudomonas acidophila* furnish a complete model of the pigment organization in the photosynthetic membrane of purple bacteria.

INTRODUCTION

The photosynthetic unit (PSU) of purple bacteria is a nanometric assembly in the intracytoplasmic membranes and consists of two types of pigment-protein complexes, the photosynthetic reaction center (RC) and light-harvesting complexes (LHs). The LHs capture sunlight and transfer the excitation energy to the RC where it serves to initiate a charge separation process (Fleming and van Grondelle, 1994; Lancaster et al., 1995; Parson and Warshel, 1995; Woodbury and Allen, 1995; Hu et al., 1998). In most purple bacteria, the PSUs contain two types of LHs, commonly referred to as B875 (LH-I) and B800-850 (LH-II) complexes according to their in vivo absorption maxima in the near-infrared (Zuber and Brunisholz, 1991). Electron micrographs have shown that LH-I surrounds directly the RC (Miller, 1982; Stark et al., 1984; Engelhardt et al., 1986; Meckenstock et al., 1992; Boonstra et al., 1994; Walz and Ghosh, 1997), forming the core of the PSU. In some species, such as *Rhodospirillum (Rs.) molischianum*, the association of LH-I and RC is so strong that LH-I cannot be separated from the RC without losing its spectral properties (Boonstra et al., 1994); in other species, such as *Rhodobacter (Rb.) sphaeroides*, pure and homogeneous LH-I complexes can be isolated (Boonstra et al., 1993). LH-II complexes surround the LH-I complex and transfer energy to the RC via LH-I (Monger and Parson, 1977; van Grondelle et al., 1994). There exist multiple LH-IIs in the PSU; the number of LH-IIs varies according to growth conditions such as light intensity and temperature (Aagaard and Sistrom, 1972; Drews and Golecki, 1995).

Excitation energy migration from light-harvesting complexes to the RC involves the chromophores, bacteriochlorophylls (BChls) and carotenoids, of all the pigment protein complexes (van Grondelle et al., 1994; Hu and Schulten, 1997a). To understand the mechanisms underlying the efficient excitation energy transfer in the bacterial PSU, structural information of each component and of the overall assembly of all the components is needed. Structures of the RC are known for *Rhodopseudomonas (Rps.) viridis* (Deisenhofer et al., 1985) as well as for *Rb. sphaeroides* (Allen et al., 1987; Ermler et al., 1994). Recently, high-resolution crystal structures of LH-II complexes from two species (*Rps. acidophila* and *Rs. molischianum*) have been determined (McDermott et al., 1995; Koepke et al., 1996). However, the structure of LH-I, the key intermediary for excitation transfer between the LH-IIs and the RC, has been lacking. We report in this article a computationally modeled structure of LH-I of *Rb. sphaeroides* and its complex with the photosynthetic reaction center. This structure provides the missing element for a complete model of the pigment organization in the bacterial PSU and opens the door to a systematic interpretation of spectroscopic observations of light harvesting in bacterial photosynthesis (van Grondelle et al., 1994; Pullerits and Sundstrom, 1996). A full account on electronic excitation transfer in the bacterial PSU is given in Hu et al., 1998.

All light-harvesting complexes of purple bacteria display a remarkably similar architecture (Zuber, 1985; Zuber and Brunisholz, 1991). The basic structural unit is a heterodimer of two short peptides, commonly referred to as α-apoprotein and β-apoprotein, noncovalently binding BChls, and carotenoids. These heterodimers form ring-shaped functional light-harvesting complexes. For LH-Is, the complex can be reversibly dissociated into the constituting subunits by addition of detergents (Ghosh et al., 1988). These structural subunits can be isolated and subsequently reconstituted back to an oligomeric LH-I (Karrasch et al., 1995; Loach and Parkes-Loach, 1995). The size of the complexes differs for LH-I and LH-II and is species dependent. LH-IIs from *Rps. acidophila* and *Rhodovulum sulfidophilum* were determined by electron microscopy (Savage et al., 1996) and

x-ray crystallography (McDermott et al., 1995) to be nonamers of the $\alpha\beta$-heterodimers. The crystal structure of LH-II from *Rs. molischianum* displayed an octamer (Koepke et al., 1996). An 8.5-Å resolution electron microscopy projection map has been determined from a two-dimensional crystal of reconstituted LH-I of *Rs. rubrum* by Karrasch et al. (1995). The projection map showed LH-I as a ring of 16 subunits; each subunit apparently corresponds to an $\alpha\beta$-heterodimer (Karrasch et al., 1995). The ring has a diameter of 116 Å with a 68-Å hole in the center that, as pointed out by Karrasch et al., is large enough to incorporate a reaction center in vivo. A recent report of an electron micrograph of a two-dimensional crystal of the LH-I—RC complex from *Rs. rubrum* further confirms the location of the RC in the center of LH-I (Walz and Ghosh, 1997).

Based on the 8.5-Å resolution projection map (Karrasch et al., 1995), several researchers constructed illustrative models of LH-I by replicating the $\alpha\beta$-heterodimer of LH-II 16 times geometrically to fill the contour peaks of the observed projection map (Papiz et al., 1996; Pullerits and Sundstrom, 1996). In this article, we present instead an all-atom model of LH-I from *Rb. sphaeroides* based on established structure prediction tools. The tools employed are the same as what we have used to predict the structure of LH-II from *Rs. molischianum* and to determine subsequently the crystal structure for the protein by means of the molecular replacement method (Hu et al., 1995; Koepke et al., 1996). We are obligated to caution the readers that our structure of LH-I represents only a model verified by low-resolution electron microscopic data. In the case of LH-II of *Rs. molischianum* (Hu et al., 1995; Koepke et al., 1996), the modeled structure served as the starting point of the analysis of x-ray diffraction data, whereas in the present case it is the final result. The ultimate test of the correctness of our LH-I model rests upon availability of high-resolution x-ray or electron microscopic data. The models of LH-I and the LH-I—RC complex presented here has been briefly outlined previously (Hu et al., 1997; Hu and Schulten, 1997a,b).

The organization of LH-I complexes around the RC is still a matter of debate. Questions have been raised as to whether the dissociation and reconstitution process employed (e.g., in Karrasch et al., 1995) introduces artifacts that render the reconstituted LH-I complexes of *Rs. rubrum* (Karrasch et al., 1995) a variant of native LH-I complexes. These concerns were alleviated by the observation that the two-dimensional crystal of the LH-I—RC complex, formed under mild crystallization conditions under which no dissociation of the LH-I—RC complex can be detected, displayed the same LH-I ring size as the reconstituted LH-I (Walz and Ghosh, 1997). Furthermore, the gross morphology of the core photosynthetic unit, which consists of a central core RC surrounded by an LH-I ring, is consistent with earlier models of the PSU for both BChl-b- and BChl-a-containing bacteria based upon electron microscopy and image processing (Miller, 1982; Stark et al., 1984; Engelhardt et al., 1986; Meckenstock et al., 1992; Boonstra et al., 1994). However, earlier models differ from the LH-I model of *Rs. rubrum* by Karrasch et al. in both number and arrangement of LH-I subunits in the ring. LH-I—RC complexes from both *Rps. viridis* (Miller, 1982; Stark et al., 1984) and *Rps. marina* (Meckenstock et al., 1992), for example, were proposed to contain 12 subunits with six-fold symmetry. However, the low resolution (40–50 Å) of images in earlier models might not be sufficient to unambiguously resolve the symmetry of the ring.

In this work, we assume that LH-I of *Rb. sphaeroides*, like LH-I of *Rs. rubrum*, is a circular aggregate of 16 subunits. The reason for choosing *Rb. sphaeroides* for our modeling work is that it is the only BChl-a-containing species for which a high-resolution crystal structure of the RC is known (Allen et al., 1987; Ermler et al., 1994). The other known bacterial RC structure is from a BChl-b-containing species, *Rps. viridis* (Deisenhofer et al., 1985), which contains an additional γ-polypeptide in the LH-I subunit (Brunisholz et al., 1985).

LH-I of *Rb. sphaeroides* contains BChl-a (Zuber and Brunisholz, 1991) as well as the carotenoids spheroidene and spheroidenone (Hunter et al., 1988) as pigments. It had been determined that the ratio of BChl to carotenoid is 1:1 in LH-I (Hunter et al., 1988). Thus, each $\alpha\beta$-heterodimer binds two BChls and two carotenoids (Zuber and Brunisholz, 1991). The α- and the β-apoprotein of LH-I from *Rb. sphaeroides* consist of 58 and 49 residues, respectively (Kiley et al., 1987; Theiler et al., 1984).

We modeled LH-I of *Rb. sphaeroides* as a hexadecamer of $\alpha\beta$-heterodimers utilizing a two-stage protocol as detailed in Materials and Methods. There are two factors that ensure validity of our approach. First, a sequence homology of the $\alpha\beta$-heterodimer of LH-I from *Rb. sphaeroides* to that of LH-II of *Rs. molischianum* (Germeroth et al., 1993) provides an opportunity to accurately model the structure of the $\alpha\beta$-heterodimer by means of homology modeling. The sequence of LH-II from *Rs. molischianum* is aligned to that of LH-I from *Rb. sphaeroides* in Fig. 1, along with sequences of other light-harvesting complexes. The α-apoprotein of the LH-II complex from *Rs. molischianum* is aligned with LH-II complexes and LH-I complexes from other photosynthetic bacteria, respectively. The β-apoproteins of both LH-Is and LH-IIs are aligned altogether. Sequence similarity of the LH-II complex from *Rs. molischianum* to both LH-IIs and LH-Is clearly demonstrates the dual characteristics of the LH-II complex from *Rs. molischianum* as first pointed out in Germeroth et al., 1993. Additional sequence analysis revealed that LH-II of *Rs. molischianum* has the highest sequence similarity to LH-Is among all the LH-IIs for which sequences are available. Second, the protocol for aggregating the $\alpha\beta$-heterodimers into a 16-fold symmetrical hexadecamer had proven successful in modeling the octameric LH-II of *Rs. molischianum*; the modeled LH-II was accurate enough to serve successfully as a probe model in the molecular replacement method (Koepke et al., 1996; Hu et al., 1995).

α-apoprotein

```
Rs. molischianum B800-850    snpkddYKIWLVINPSTWLPVIWIVATVVAIAVHAAVLAAPGFNWIALGAAKsaak----
Rc. gelatinosus DSM 149 B870 -----mWRIWRLFDPMRAMVAQAVFLLGLAVLIHLMLLGTNKFNWLDGAKKApvasa---
Rs. rubrum B870              -----mWRIWQLFDPRQALVGLATFLFVLALLIHFILLSTERFNWLEGASTQpvqts---
Rb. capsulatus B870          --mskfYKIWLVFDPRRVFVAQGVFLFLLAVLIHLILLSTPAFNWLTVATAKhgyvaaaq
Rb. sphaeroides B870         --mskfYKIWMIFDPRRVFVAQGVFLFLLAVMIHLILLSTPSYNWLEISAAKynrvavae
Rps. marina B880             -----mWKVWLLFDPRRTLVALFTFLFVLALLIHFILLSTDRFNWMQGAPTApaqts---
Rp. viridis B1015            eyrtasWKLWLILDPRRVLTALFVYLTVIALLIHFGLLSTDRLNWWEFQRGLpkaa----

Rs. molischianum B800-850    snpkddYKIWLVINPSTWLPVIWIVATVVAIAVHAAVLAAPGFNWIALGAAKsaak----
Rp. viridis B1015            eyrtasWKLWLILDPRRVLTALFVYLTVIALLIHFGLLSTDRLNWWEFQRGLpkaa----
Rc. gelatinosus DSM 149 B800-850 ---mnQGKVWRVVKPTVGVPVYLGAVAVTALILHGGLLAKTDWFGaywnggkkaaaa---
Rb. sphaeroides 2.4.1 B800-850   ---mtNGKIWLVVKPTVGVPLFLSAAVIASVVIHAAVLTTTTWLPayyqgsaavaae---
Rb. capsulatus B800-850          ---mnNAKIWTVVKPSTGIPLILGAVAVAALIVHAGLLTNTTWFAnywngnpmatvvava
Rps. acidophila Ac70.50 B800-850 ---mnQGKIWTVVNPSVGLPLLLGSVTVIAILVHAAVLSHTTWFPaywqgglkkaa----
Rps. palustris 2.6.1 B800-850    ---mnQGRIWTVVNPGVGLPLLLGSVTVIAILVHYAVLSNTTWFPkywngatvaapaaa-
```

β-apoprotein

```
Rs. molischianum B800-850       ----AERSLSGLTEEEAIAVHDQFKTTFSAFIILAAVAHVLVWVWKPWf--------
Rc. gelatinosus DSM 149 B870    --aeRKGSISGLTDDEAQEFHKFWVQGFVGFTAVAVVAHFLVWVWRPWl--------
Rs. rubrum B870                 --evKQESLSGITEGEAKEFHKIFTSSILVFFGVAAFAHLLVWIWRPWvpgpngys-
Rb. capsulatus B870             -adkNDLSFTGLTDEQAQELHAVYMSGLSAFIAVAVLAHLAVMIWRPWf--------
Rb. sphaeroides B870            -adkSDLGYTGLTDEQAQELHSVYMSGLWPFSAVAIVAHLAVYIWRPWf--------
Rps. marina B880               aeidRPVSLSGLTEGEAREFHGVFMTSFMVFIAVAIVAHILAWMWRPWipgpegia-
Rp. viridis B1015               --adLKPSLTGLTEEEAKEFHGIFVTSTVLYLATAVIVHYLVWTAKPWiapipkgwv
Rc. gelatinosus DSM 149 B800-850 addaNKVWPSGLTTAEAEELQKGLVDGTRIFGVIAVLAHILAYAYTPWlh-------
Rb. sphaeroides 2.4.1 B800-850  -ddlNKVWPSGLTVAEAEIVHKQLILGTRVFGGMALIAHFLAAAATPWlg-------
Rb. capsulatus B800-850         -mtdDKAGPSGLSLKEAEEIHSYLIDGTRVFGAMALVAHILSAIATPWlg-------
Rps. acidophila Ac70.50 B800-850 --adDVKGLTGLTAAESEELHKHVIDGTRVFFVIAIFAHVLAFAFSPWlh-------
Rps. palustris 2.6.1 B800-850   addpNKVWPTGLTIAESEELHKHVIDGSRIFVAIAIVAHFLAYVYSPWlh-------
```

FIGURE 1   Sequence alignment of the α- and β-apoproteins of the LH-II complex of *Rs. molischianum* with α- and β-apoproteins of LH-II and LH-I complexes from other photosynthetic bacteria. Bold and shadow fonts indicate highly and nearly conserved residues, respectively. For the α-apoprotein, the LH-II complex from *Rs. molischianum* is aligned with LH-II complexes from other photosynthetic bacteria on the top panel and with LH-I complexes on the bottom panel. Alignment was done using the program MACAW (multiple alignment construction and analysis workbench) (Schuler et al., 1991).

MATERIALS AND METHODS

LH-I of *Rb. sphaeroides* had been modeled as a hexadecamer of αβ-heterodimers utilizing a two-stage protocol as described previously (Hu et al., 1995, 1996; Koepke et al., 1996). In a first step, the αβ-heterodimer was constructed by means of homology modeling using the αβ-heterodimer of LH-II of *Rs. molischianum* as a template. Our protocol emphasizes both sequence homology and secondary structure identity as search criteria in choosing templates for homology modeling. As shown in Fig. 2, the sequence of LH-I of *Rb. sphaeroides* is homologous to that of LH-II of *Rs. molischianum*. For the aligned LH-I core segment α-Tyr-5 to α-Lys-50, the α-apoproteins are 30% identical and 56% homologous; for the aligned LH-I core segment β-Thr-10 to β-Phe-49, the β-apoproteins are 40% identical and 67% homologous. A consensus assignment for the secondary structure of the α- and β-apoprotein of LH-I of *Rb. sphaeroides*, listed in Fig. 2, was derived by means of multiple secondary structure prediction methods (Engelman et al., 1986; Persson and Argos, 1994; Geourjon and Deleage, 1994; Holley and Karplus, 1991) as had been done in the case of LH-II of *Rs. molischianum* (Koepke et al., 1996; Hu et al., 1995, 1996). Also listed in Fig. 2 are the secondary structure identities of

α-apoprotein

```
Prediction[a]            CCCCCCCCCCCCHHHHHHHHHHHHHHHHHHHHHHHHHCCCCCCHHHHHHHHHHHHHHHHH
Rb. sphaeroides          MSKFYKIWMIFDPRRVFVAQGVFLFLLAVMIHLILLSTPSYNWLEISAAKYNRVAVAE
Alignment                    YKIW++ +P          +     ++A+  +H   +L+  P  +NW+ +  AAK
Rs. molischianum   SNPKDDYKIWLVINPSTWLPVIWIVATVVAIAVHAAVLAAPGFNWIALGAAKSAAK
X-Ray[b]                 CCCCC333333CCCHHHHHHHHHHHHHHHHHHHHHHHHHHHHCCCCCCHHHHHHHHHHHHC
```

β-apoprotein

```
Prediction[a]              CCCCCCCCCHHHHHHHHHHHHHHHHHHHHHHHHHHHHHHHHHHHHHHHCCC
Rb. sphaeroides          MADKSDLGYTGLTDEQAQELHSVYMSGLWLFSAVAIVAHLAVYIWRPWF
Alignment                       +GLT+E+A  +H + +     F  +A VAH+ V++W+PWF
Rs. molischianum         AERSLSGLTEEEAIAVHDQFKTTFSAFIILAAVAHVLVWVWKPWF
X-Ray[b]                 CCCCCCCCCHHHHHHHHHHHHHHHHHHHHHHHHHHHHHHHHHHHHCCCC
```

FIGURE 2   Sequence alignment of α- and β-apoproteins of LH-I from *Rb. sphaeroides* and of LH-II from *Rs. molischianum* based on BLAST (Altschul et al., 1990), along with secondary structure information. [a]Secondary structure derived from consensus assignment for LH-I employing hydropathy analysis (Engelman et al., 1986), multiple sequence alignment propensity analysis (Persson and Argos, 1994), SOPM (Geourjon and Deleage, 1994), and Holley-Karplus analysis (Holley and Karplus, 1991). H, helix; E, β-sheet; C, coil; 3, three-turn helix. [b]Secondary structure of LH-II of *Rs. molischianum* as determined by the method of Kabsch and Sander (1983) from the coordinates of LH-II of *Rs. molischianum* (Koepke et al., 1996).

the crystal structure of LH-II of *Rs. molischanum* (Koepke et al., 1996). The secondary structure identities of the two proteins are in agreement. We concluded then that the αβ-heterodimer of LH-II of *Rs. molischanum* is a good template for LH-I of *Rb. sphaeroides*.

Consequently, the β-apoprotein of LH-I was modeled as a single membrane-spanning helix as in LH-II. The α-apoprotein of LH-I was modeled as a membrane-spanning helix linked to a short helical segment at the amino terminus and to an interfacial amphiphilic helix at the carboxy terminus. The carboxyl-terminal sequence of the α-apoprotein of LH-I from *Rb. sphaeroides* is longer than that of LH-II from *Rs. molischanum*. Secondary structure analysis indicates that the extra residues have a high propensity to form an α-helix (see Fig. 2) and should extend the interfacial amphiphilic helix.

The two conserved histidines near the carboxy termini of the α- and β-apoprotein were widely considered as ligands of the two B875 BChls (Zuber and Brunisholz, 1991; Olsen and Hunter, 1994). Despite a large difference in absorption maxima (875 versus 850 nm), LH-I of *Rb. sphaeroides* and LH-II of *Rs. molischanum* show strikingly similar resonance Raman spectra (Germeroth et al., 1993), which are known to be sensitive to hydrogen bond patterns of the 2-acetyl and the 9-keto groups of BChl-a (Robert and Lutz, 1985; Germeroth et al., 1993). Accordingly, the BChl-a binding site of LH-I of *Rb. sphaeroides* should be similar to that of LH-II from *Rs. molischanum*. The BChls were placed into the αβ-heterodimer of LH-I at positions analogous to those in LH-II from *Rs. molischanum*, and so was the spheroidene. Only one spheroidene per αβ-heterodimer was included in the model.

In a second step, the αβ-heterodimers were aggregated into a circular hexadecameric complex by means of molecular dynamics simulations and energy minimization under the constraint of a 16-fold symmetry axis. An iterative protocol consisting of multiple dynamics and minimization cycles, shown in Fig. 3, was employed to optimize the hexadecamer structure. Each cycle started with a 200-step rigid body minimization (with the entire protomer as a rigid body), followed by a 2.5-ps rigid body dynamics run at 600 K, then a 5-ps constrained molecular dynamics run at 300 K, ending with a 200-step constrained Powell minimization. The positions of all C_α atoms were fixed (constrained) during the last two steps of the cycle. The radius of the hexadecamer was monitored to detect convergence. The

iterative process was terminated when the final radii at the end of two consecutive runs differed by less than 0.10 Å. At the end, the hexadecamer was minimized again with the Powell algorithm until it converged or until a limit of 700 cycles was reached. This protocol, energy minimizations perturbed by successive molecular dynamics equilibration, constitutes a simulated annealing procedure.

The molecular dynamics simulations and energy minimizations were carried out using the program X-PLOR (Brünger, 1996). In all simulations, LH-I was placed in a vacuum as the vacuum environment is believed to be similar to a lipid bilayer in terms of hydrophobicity. The Engh and Huber parameter set (Engh and Huber, 1991) was used for the protein. The parameter file used for BChl-a is the same as in Koepke et al., 1996; the parameter set for the spheroidene was constructed with the program QUANTA (MSI, 1994) using the CHARMm (Brooks et al., 1983) force field.

In the above, we placed the α-apoprotein on the inside and the β-apoprotein on the outside of the LH-I ring in analogy to LH-IIs (McDermott et al., 1995; Koepke et al., 1996). This is apparently consistent with surface-specific iodination of both the photosynthetic membranes and the isolated PSU (Jay et al., 1984); the work indicated that β-apoprotein of *Rps. viridis* is situated on the outside of the LH-I ring.

Five initial structures for the hexadecamer were built, with initial radii of 51, 53, 55, 59, and 81 Å. All five hexadecamers converged in the optimization procedure (see Fig. 3) to a radius of 54 Å as defined through the central axes of the outer helical ring. The root mean square (rms) deviation of C_α atoms among all five optimized models ranged from 0.3 to 0.7 Å. The structure with the lowest conformational energy was chosen as the final model. We note that all five models can be considered essentially the same as they show rms deviations in a range (0.3–0.7 Å) compatible with that of high-resolution crystal structures of proteins determined at different laboratories (Flores et al., 1993).

The modeled LH-I complex was subsequently docked to the photosynthetic reaction center to form the LH-I—RC complex. Coordinates of RC were taken from the 2.65-Å resolution structure of the photosynthetic reaction center of *Rb. sphaeroides* [Protein Data Bank accession number 1PCR] as published previously (Ermler et al., 1994). Two approaches had been attempted in searching for the minimal energy conformation of the LH-I—RC complex, i.e., a rigid body minimal energy search and a constrained conformational search. In the former approach, the RC structure was placed inside the LH-I ring and was allowed to rotate and translate as a rigid body. In the latter approach, both LH-I and RC were treated as rigid bodies and two constraints were enforced in the search: first, the planes of tryptophan residues in both the RC and LH-I (see Results) were constrained to be parallel to the plane of the membrane, i.e., the *x*, *y* plane; second, the pseudo 2-fold symmetry axis of the RC was aligned with the 16-fold symmetry axis of LH-I. As a result, only two degrees of freedom for the rigid body movement of the RC inside the LH-I ring remained: translation along the *z* axis (*Z*) and rotation around the symmetry axis (θ). Shown in Fig. 4 is the energy landscape governing the constrained conformational search. The interaction energy between LH-I and RC is a sensitive function of *Z* and θ. A unique minimum, actually shown as a maximum in Fig. 4 *a*, exists for the LH-I—RC complex at *Z* = 0 and θ = 4.6°. For the stated *Z* value (0), the planes of tryptophans of LH-I and RC are co-planar. None of the rigid-body minimal energy searches initiated at various initial configurations yielded a minimum as low as the one determined by the constrained conformational search.

RESULTS

LH-I of *Rb. sphaeroides*

The modeled structure of LH-I of *Rb. sphaeroides* is presented in Fig. 5. Sixteen αβ-heterodimers form a hollow cylinder with the α-apoprotein positioned to the inside and the β-apoprotein to the outside. The diameter of the inner helical ring is 78 Å as defined through the central axes of
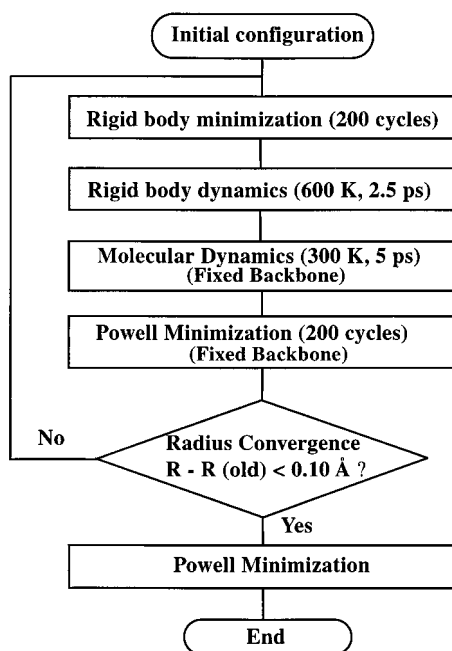

FIGURE 3   Optimization protocol for aggregating the hexadecameric LH-I complex. A 16-fold rotational symmetry was enforced throughout the simulation.
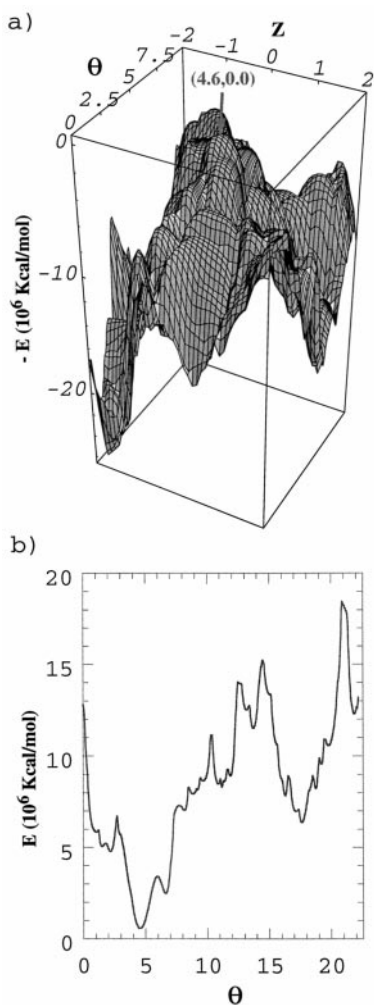
FIGURE 4 Energy diagrams for the constrained conformational search of the LH-I–RC complex. (*a*) Interaction energy between LH-I and RC as a function of Z and θ. Z represents translation of the RC along the z axis, and θ stands for rotation of the RC along its pseudo 2-fold symmetry axis. Due to the 16-fold symmetry of LH-I, θ is limited to the interval [0°, 22.5°]. The sign of the interaction energy E is reversed in the plot for a better view. Z is in angstroms and θ is in degrees. (*b*) Interaction energy between LH-I and RC as a function of θ for $Z = 0$.

the helices, and that of the outer helical ring measures 108 Å. The overall diameter of the LH-I complex is 118 Å.

An x-ray projection map of the modeled hexadecameric complex was generated utilizing the program X-PLOR (Brünger, 1996) and the program NPO in the CCP4 package (CCP4, 1994). The calculated x-ray projection map of LH-I of *Rb. sphaeroides* was superimposed onto the measured 8.5-Å electron microscopy projection map of LH-I of *Rs. rubrum* as published previously (Karrasch et al., 1995). The two independently determined maps are presented in Fig. 5 *c* and exhibit good agreement. Peaks of the contours display a perfect match, which indicates that the membrane-spanning helices in the model are positioned correctly. We note that the calculated map displays a denser projection density for the outer helices than the experimentally measured map. It is important to realize that the experimental projection

map that we used for comparison is a rotationally filtered map (Fig. 6a in Karrasch et al., 1995) arrived at by imposing 16-fold rotational symmetry. The unfiltered map (Fig. 4 in Karrasch et al., 1995) displayed densities for the inner and outer helices with approximately the same number of contours in a way that is quite similar to our calculated projection map. The minor difference in density in the region between the inner and outer helices may be attributed to differences in the length of the two termini of the α-apoprotein of LH-I of *Rb. sphaeroides* and of *Rs. rubrum* (see Fig. 1).

Shown in Fig. 6 *a* is a stereo diagram of the modeled structure of a single $\alpha\beta$-heterodimer of LH-I, which consists of the α- and the β-apoprotein binding a pair of B875 BChls and a carotenoid molecule, spheroidene. Residues α-Asp12 to α-Thr38 of the α-apoprotein form a straight α-helix that spans the photosynthetic membrane and is oriented perpendicular to the membrane within 1°. In addition to this helix, the α-apoprotein possesses also two short helical segments at both the amino and the carboxy terminus. The carboxyl-terminal interfacial α-helix is 16 residues long (α-Asn42 to α-Ala57) and amphiphilic. Residues β-Thr13 to β-Arg46 of the β-apoprotein also form a trans-membrane α-helix, however, with a tilt of $\sim 8°$. We note that there exists an uncertainty in the amino-terminal region of the α-apoprotein in our LH-I model, which arises from the fact that the amino-terminal region of the α-apoprotein in LH-I is no longer the ligation site of a BChl molecule due to lack of the B800 BChl in LH-I in comparison with LH-II. Also, spheroidene is simply placed in a binding pocket in analogy to the binding site of lycopene in LH-II of *Rs. molischianum* (Koepke et al., 1996).

The B875 BChls are sandwiched between the helices of the α- and β-apoproteins; they are oriented perpendicular to the plane of the membrane. The Mg–Mg distance between neighboring B875 BChls is 9.2 Å within the $\alpha\beta$-heterodimer and 9.3 Å between neighboring heterodimers. We denote by B875a the B875 BChl ligated to the α-apoprotein and by B875b the B875 BChl ligated to the β-apoprotein.

The binding site for the B875 BChls in one $\alpha\beta$-heterodimer is depicted in Fig. 6 *b*. The central Mg atoms of the BChls are ligated to two conserved histidines, α-His32 and β-His39. The distance between the Mg atom of B875a and the $N_{\epsilon 2}$ atom of α-His32 is 2.4 Å and that between the Mg atom of B875b and the $N_{\epsilon 2}$ atom of β-His39 measures also 2.4 Å. The 2-acetyl carboxyl oxygen (O_{BB}) atoms of the two BChl molecules are hydrogen bonded to the $N_{\epsilon 1}$ atom of α-Trp43 and the $N_{\epsilon 1}$ atom of β-Trp48, respectively. The hydrogen bond distance measures 2.9 Å for the former and 2.7 Å for the latter. The suggested hydrogen bonds are consistent with resonance Raman spectra and the observed absorption spectra shift of LH-I of *Rb. sphaeroides* and its mutants (Olsen et al., 1994; Sturgis et al., 1997).

In analogy to LH-II of *Rs. molischianum* (Koepke et al., 1996; Hu et al., 1997), the two histidine residues α-His32 and β-His39, which bind the central Mg atoms of the B875 BChls, appear to be involved also in hydrogen bonding of
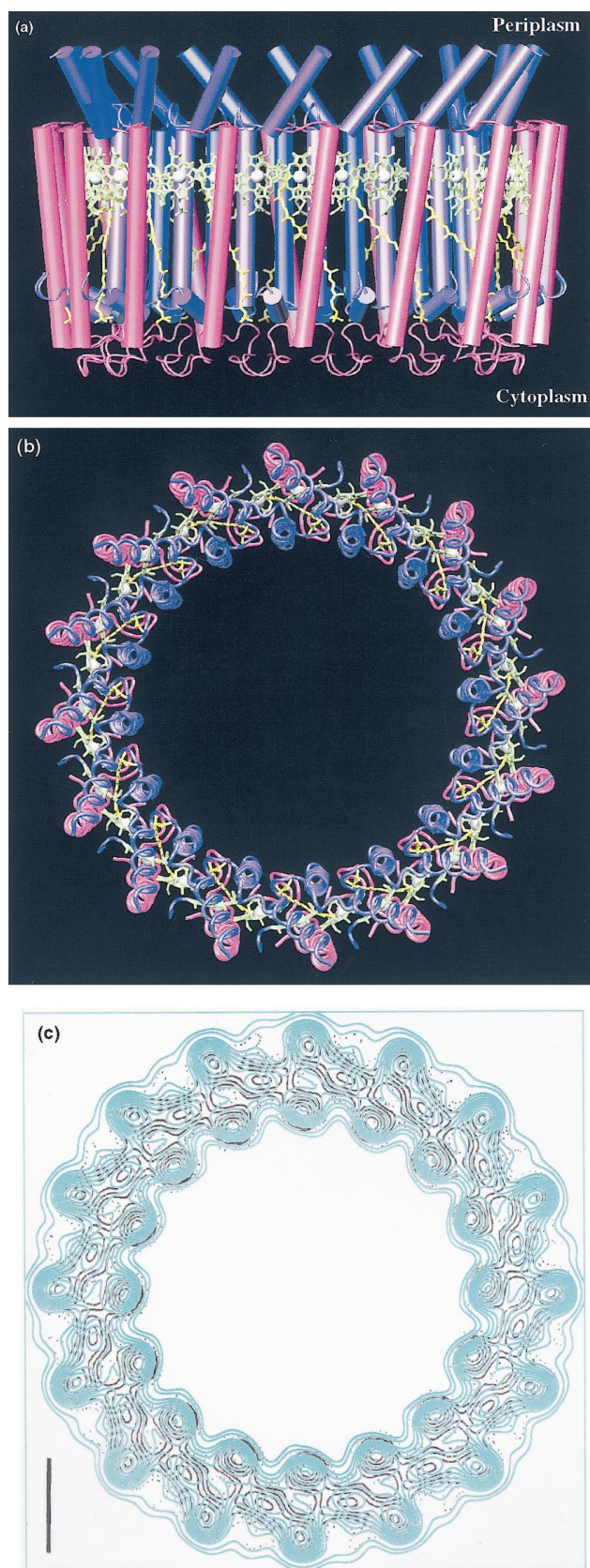
FIGURE 5   Modeled structure of LH-I of *Rb. sphaeroides*. (a) Side view. α-Helical segments are represented as cylinders with α-apoproteins in blue and β-apoproteins in magenta. The BChl-a molecules are in green with their phytyl tails truncated for clarity and with Mg atoms as white spheres.

the 9-keto group of the B875 BChls. As depicted in Fig. 6 *b*, the distance between the $N_{\delta 1}$ atom of α-His32 and the 9-keto oxygen of B875b BChl is 3.6 Å, and the distance between the $N_{\delta 1}$ atom of β-His39 and the 9-keto oxygen of B875a BChl is 3.5 Å. We note that a distance of 3.5 Å between donor and acceptor is not favorable for formation of a strong hydrogen bond.

The suggested hydrogen bonds, however, are supported by the observed resonance Raman spectra of different mutants of LH-I of *Rb. sphaeroides* (Olsen et al., 1997). Vibrations in the $1600–1700 \text{ cm}^{-1}$ region are known to be associated with the stretching modes of the conjugated carbonyl group, i.e., the 2-acetyl and the 9-keto groups of BChl-a (Robert and Lutz, 1985). The peak frequency for the unbounded 9-keto group is $\sim 1700 \text{ cm}^{-1}$. The peak shifts by -40 cm^{-1} upon hydrogen bonding. This characteristic peak for the hydrogen-bonded 9-keto group has been observed in the resonance Raman spectra of LH-I from *Rb. sphaeroides* (Olsen et al., 1994, 1997). When all of the potential hydrogen-bonding side chains, except the Mg-binding histidines, in the immediate surroundings of the 9-keto group were mutated, the characteristic hydrogen-bonded 9-keto Raman peak was not affected. However, when the central Mg-binding histidine residue of the β-apoprotein was mutated, the characteristic Raman peak was attenuated substantially (Olsen et al., 1997), which suggests that the central Mg-binding histidine residues also formed hydrogen bonds with the 9-keto groups of the B875 BChls in LH-I. Each B875 BChl is then noncovalently bound to three side-chain atoms of the α- or β-apoprotein such that the orientation of the B875 BChls is spatially well defined. This spatial stability may contribute to an overall geometrical rigidity of the circular form of LH-I and may have implications for the mechanism of light energy transfer in that the transition dipole moments of the BChls are maintained in a well ordered arrangement.

LH-I—RC complex

A constrained rigid-body minimal energy search was carried out (see Materials and Methods) to place the photosynthetic reaction center inside the LH-I ring. A unique, energetically optimal configuration was reached. Fig. 7 *a* presents the LH-I—RC complex in van der Waals representation demonstrating a tight fit of RC inside LH-I.

Spheroidenes are in yellow. (*b*) Top view with carboxy termini pointing upward; the apoproteins are represented as C_α tracing tubes. Same color coding as in *a*. (Produced with the program VMD (Humphrey et al., 1996).) (*c*) Superposition of simulated x-ray projection map (cyan) of LH-I of *Rb. sphaeroides* onto the measured 8.5-Å electron microscopic projection map (black) of LH-I of *Rs. rubrum* (Karrasch et al., 1995). The x-ray projection map was calculated from structure factors generated from the coordinates of the modeled LH-I structure of *Rb. sphaeroides*, with carboxy termini at top, to 8.5-Å resolution. Contours are in steps of $0.3 \times$ rms density; scale bar represents 20 Å. The overall dimension of the cell is 120×120 Å.

FIGURE 6 (*a*) Stereo view of the αβ-heterodimer of LH-I of *Rb. sphaeroides*. Apoproteins are drawn as C$_\alpha$ tracing with α-apoprotein in cyan and β-apoprotein in magenta. BChls are in green, and spheroidene is in yellow. (*b*) Stereo view of the B875 bacteriochlorophylls and their binding partners in an αβ-heterodimer. The α- and β-apoproteins (blue and magenta, respectively) in the nearby region are shown in tube representation. Dashed lines represent metal and hydrogen bonds; numbers indicate distances in angstroms. Produced with the program VMD (Humphrey et al., 1996).
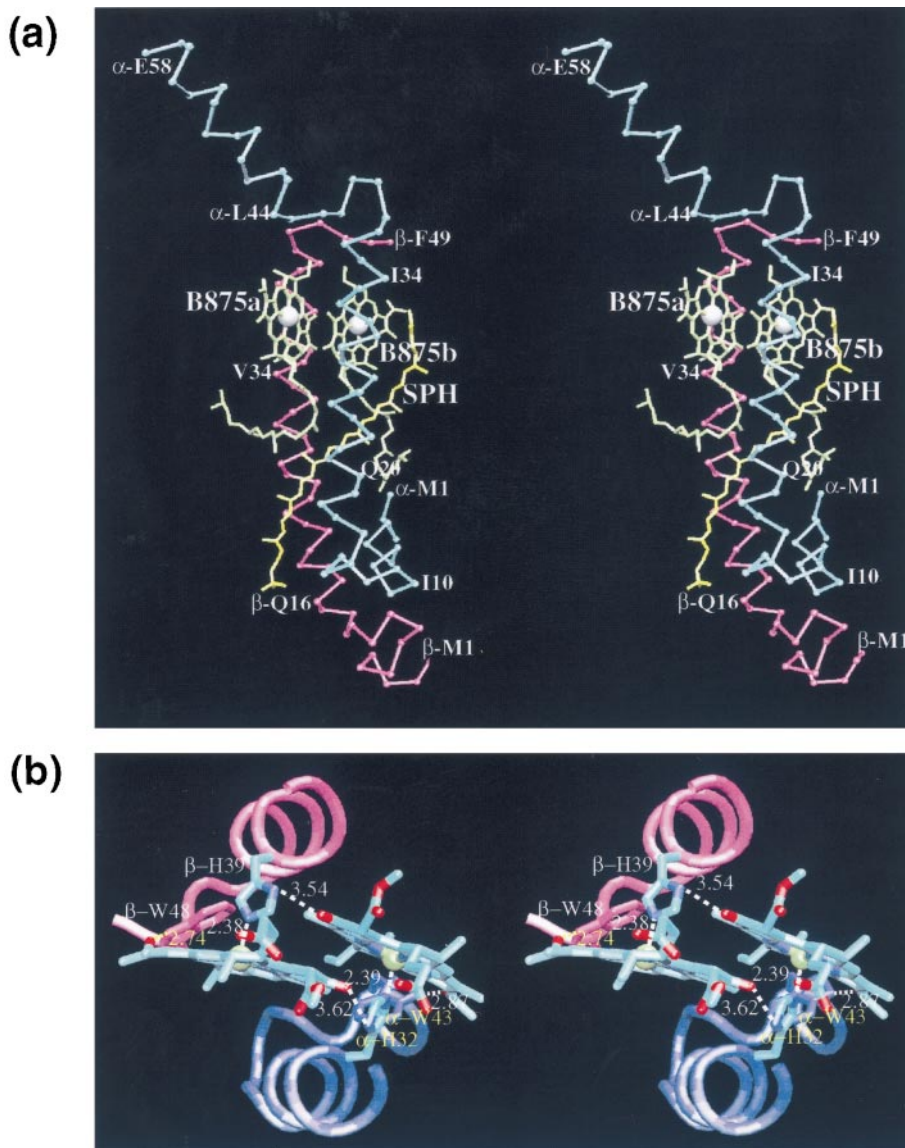
A striking feature of the LH-I—RC complex is the arrangement of tryptophans situated on the periplasmic side. Fig. 7 *b* shows the tryptophan residues in the LH-I—RC complex. A plane of tryptophans common to both RC and LH-I can be recognized. The presence of aromatic residues (mainly tryptophan and tyrosine) flanking membrane-spanning segments has been well documented for bacterial porins (Cowan et al., 1992; Weiss and Schulz, 1992), the bacterial reaction centers (Schiffer et al., 1992), and eukaryotic membrane proteins (Landolt-Marticorena et al., 1993). Such a plane of tryptophans is also found in the crystal structure of LH-II of *Rs. molischianum* (Koepke et al., 1996).

Depicted in Fig. 7 *c* is the arrangement of BChls in the LH-I—RC complex. The plane of the ring of BChls in LH-I encompasses also the reaction center special pair (P$_A$ and P$_B$) and the so-called accessory bacteriochlorophylls (B$_A$ and B$_B$). Table 1 lists coordinates (*x*, *y*, *z*) of the central Mg atoms of BChls, along with unit vectors (U_x, U_y, U_z) for the

Q_y transition dipole moments of BChls as defined by the long *Y* axis of BChl that connects the N atom of pyrrol I and the N atom of pyrrol III (Gouterman, 1961). The closest distance between the central Mg atom of the RC special pair (bacteriochlorophylls P$_A$ and P$_B$) and the Mg atom of the BChls in LH-I is 42.6 Å. The distance between the Mg atom of the accessory BChl (bacteriochlorophylls B$_A$ and B$_B$) and the LH-I BChls is shorter, the nearest distance measuring 35.7 Å.

Pigment organization in the PSU

As discussed above, the planes of tryptophans in both the LH-I—RC complex and the LH-II complex are located in the lipid-water interfacial region and, thereby, align the pigment-protein complexes of the PSUs. Fig. 8 presents LH-II in contact with the LH-I—RC complex as aligned by the planes of tryptophans: the LH-I—RC complex of *Rb.*
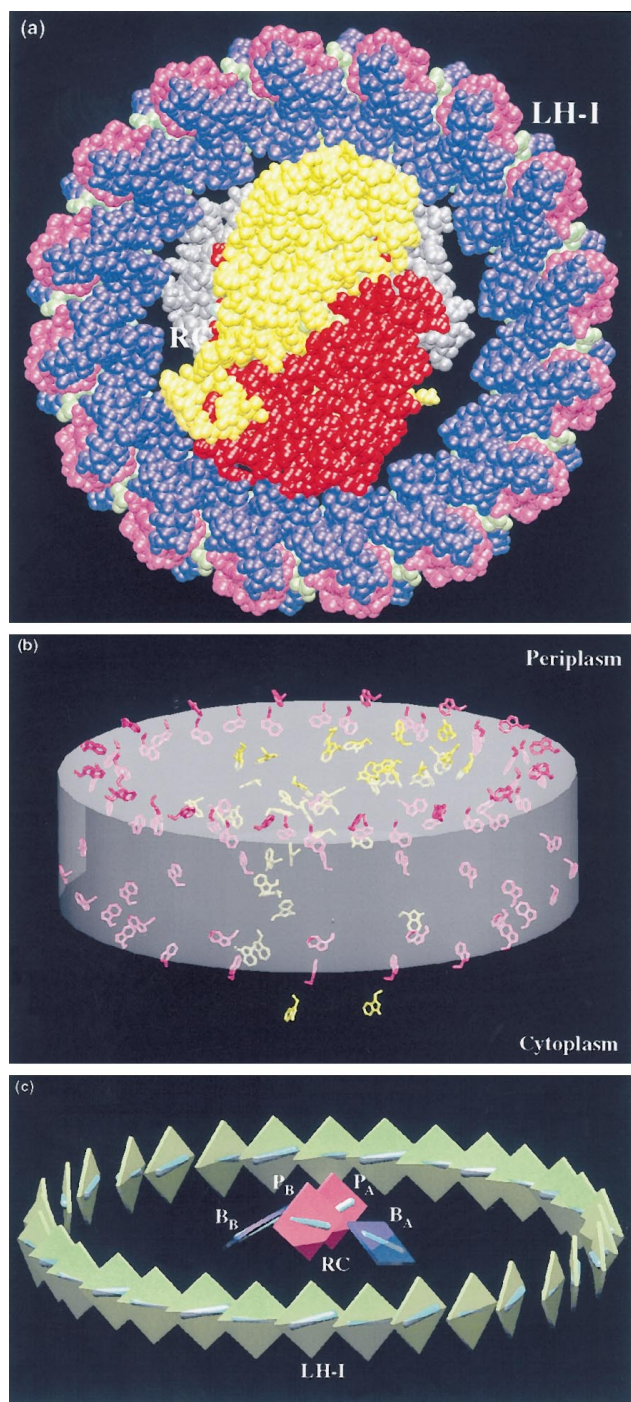
FIGURE 7 Structure of the LH-I—RC complex. (*a*) van der Waals representations of the complex with the periplasmic side on top. The L, M, and H subunits of the RC are shown in yellow, red, and gray; the α-apoprotein and the β-apoprotein of the LH-I are in blue and magenta, and the BChls are in green. (*b*) Distribution of tryptophan residues in the LH-I—RC complex. All tryptophans of the RC (yellow) and LH-I (magenta) are shown. The planes of the cylinder are parallel to the plane of the membrane. (*c*) Arrangement of BChls in the LH-I—RC complex. The BChls are represented as squares with B875 BChls of LH-I in green and the special pair (P_A and P_B) and the accessory bacteriochlorophylls (B_A and B_B) of the RC in red and blue, respectively; cyan bars represent Q_y transition moments of bacteriochlorophylls as defined by the vector connecting the N atom of pyrrol I and the N atom of pyrrol III (Gouterman, 1961). Produced with the program VMD (Humphrey et al., 1996).

sphaeroides shown has been modeled in this work, and LH-II is from *Rs. molischianum* as described previously (Koepke et al., 1996). As there exists, currently, no direct evidence that indicates LH-II of *Rb. sphaeroides* is an octamer or nonamer, we simply substitute the crystal structure of LH-II of *Rs. molischianum* (Koepke et al., 1996) for LH-II of *Rb. sphaeroides* for the purpose of illustration. Such an assembly can be viewed as the most basic PSU. Both LH-I and LH-II rings of BChls are positioned near the periplasmic side of the photosynthetic apparatus. More importantly, the B850 BChls of LH-II and the B875 BChls of LH-I are all exactly co-planar. The shortest Mg–Mg distance between B875 BChls of LH-I and B850 BChls of LH-II measures ~22 Å.

DISCUSSION

In this article, we modeled an atomic structure for LH-I of *Rb. sphaeroides* by means of homology modeling, molecular dynamics simulations, and energy minimization. Our goal was to establish an atomic model of the pigment organization in the bacterial PSU to guide and stimulate further spectroscopic and biochemical experiments (Wu et al., 1997; Pullerits and Sundstrom, 1996; van Grondelle et al., 1994; Olsen et al., 1997). To better achieve this goal, we provide readers with an assessment of the quality of the model.

The correctness of LH-I model of *Rb. sphaeroides* depends on two key factors, i.e., the assumption of LH-I as a hexadecamer of αβ-heterodimers and the suitability of the modeling protocol. The former assumption is based on the observation that the reconstituted LH-I complex of *Rs. rubrum* is a hexadecamer. As shown in Fig. 1, the α- and β-apoproteins of LH-I of *Rb. sphaeroides* are highly homologous to those of LH-I of *Rs. rubrum*. More importantly, our modeling work demonstrated that 16 is the smallest number of αβ-heterodimers that can form a circular aggregate around the RC. There exist, however, certain differences between the bacterium *Rb. sphaeroides* and *Rs. rubrum*. *Rhodospirillum rubrum* contains, for example, only an LH-I complex in the PSU whereas *Rb. sphaeroides* possesses both LH-I and LH-II complexes. *Rhodobacter sphaeroides* contains an additional PufX protein (Farchaus and Oesterhelt, 1989; Lee et al., 1989) that is absent in *Rs. rubrum*. A number of studies have shown that strains of *Rb. sphaeroides* that lack the *PufX* gene are incapable of photosynthetic growth (Farchaus et al., 1990; McGlynn et al., 1994). It has been demonstrated that the PufX protein is involved, directly or indirectly, in ubiquinone/ubiquinol exchange between the RC and the cytochrome bc_1 complex (Barz et al., 1995). However, $PufX^-$ mutants in *Rb. sphaeroides* still produce intact LH-I complexes with a normal absorption maximum at 875 nm (McGlynn et al., 1994), which is an indication that PufX is not essential for LH-I formation and justifies a model of LH-I lacking PufX.

The applicability of the modeling protocol to the circular aggregate has been tested by the successful modeling of the

TABLE 1 Structural data for the LH-I–RC complex

|		x	y	z	U_x	U_y	U_z
LH-I	1	44.706	−12.591	71.986	0.634	0.760	0.147
	2	47.167	−3.677	72.184	−0.452	−0.886	0.098
	3	46.122	5.475	71.986	0.295	0.944	0.147
	4	44.984	14.653	72.184	−0.079	−0.992	0.098
	5	40.515	22.709	71.986	−0.089	0.985	0.147
	6	35.952	30.752	72.184	0.307	−0.947	0.098
	7	28.741	36.485	71.986	−0.459	0.876	0.147
	8	21.448	42.169	72.184	0.646	−0.757	0.098
	9	12.591	44.706	71.986	−0.760	0.634	0.147
	10	3.677	47.167	72.184	0.886	−0.452	0.098
	11	−5.475	46.122	71.986	−0.944	0.295	0.147
	12	−14.653	44.984	72.184	0.992	−0.079	0.098
	13	−22.709	40.515	71.986	−0.985	−0.089	0.147
	14	−30.752	35.952	72.184	0.947	0.307	0.098
	15	−36.485	28.741	71.986	−0.876	−0.459	0.147
	16	−42.169	21.448	72.184	0.757	0.646	0.098
	17	−44.706	12.591	71.986	−0.634	−0.760	0.147
	18	−47.167	3.677	72.184	0.452	0.886	0.098
	19	−46.122	−5.475	71.986	−0.295	−0.944	0.147
	20	−44.984	−14.653	72.184	0.079	0.992	0.098
	21	−40.515	−22.709	71.986	0.089	−0.985	0.147
	22	−35.952	−30.752	72.184	−0.307	0.947	0.098
	23	−28.741	−36.485	71.986	0.459	−0.876	0.147
	24	−21.448	−42.169	72.184	−0.646	0.757	0.098
	25	−12.591	−44.706	71.986	0.760	−0.634	0.147
	26	−3.677	−47.167	72.184	−0.886	0.452	0.098
	27	5.475	−46.122	71.986	0.944	−0.295	0.147
	28	14.653	−44.984	72.184	−0.992	0.079	0.098
	29	22.709	−40.515	71.986	0.985	0.089	0.147
	30	30.752	−35.952	72.184	−0.947	−0.307	0.098
	31	36.485	−28.741	71.986	0.876	0.459	0.147
	32	42.169	−21.448	72.184	−0.757	−0.646	0.098
RC	P_A	−3.402	−2.049	68.512	−0.379	−0.860	−0.342
	P_B	3.317	2.301	68.262	0.371	0.871	−0.321
	B_A	3.369	−9.909	72.059	0.208	0.854	−0.476
	B_B	−2.852	10.539	70.886	−0.300	−0.870	−0.391

Coordinates (x, y, z) of the central Mg atoms of BChls and unit vectors (U_x, U_y, U_z) for the Q_y transition dipole moments of BChls as defined by the long Y axis of BChl that connects the N atom of pyrrol I and the N atom of pyrrol III (Gouterman, 1961).

LH-II complex from *Rs. molischianum* to produce a tertiary structure for the protein that served as a probe model in the molecular replacement method (Koepke et al., 1996; Hu et al., 1995). In modeling the structure of LH-I from *Rb. sphaeroides*, no input was taken from the electron density projection map of LH-I from *Rs. rubrum*. The fact that the modeled structure yielded a calculated electron density projection map that agreed with the measured electron density projection map of LH-I from *Rs. rubrum* without adjustment is an indication that the helical segments in the modeled structure are positioned properly.

The modeling of LH-I and the LH-I—RC complex establishes an atomic model of pigment organization of the bacterial PSU. Two significant features of the pigment organization, as depicted in Fig. 8, are 1) the ring-like BChl aggregates within LH-II and LH-I and 2) the co-planar arrangement of these aggregates and the BChls in RC. Such planar pigment organization appears to be optimal for the function of the light-harvesting complexes, i.e., to transfer excitation energy to the RC.

A combination of spatial and energetic order supports this function: the peripheral components absorb at higher energy, and the core components absorb at lower energy. The LH-II complex, which surrounds LH-I, absorbs light at the highest energy (at 500 nm by carotenoids and at 800 nm and 850 nm by BChls). The electronic excitation of carotenoids and B800 BChls is transferred rapidly (<1 ps) in LH-II to a circular aggregate of 16 BChls absorbing at 850 nm (Shreve et al., 1991; Joo et al., 1996). The circular aggregate of B875 BChls in LH-I, which surrounds the RC, absorbs at 875 nm and, thereby, can trap the electronic excitation of LH-II. The energy cascade described naturally funnels energy from the outer regions of the antenna complex to the RC. The RC accepts excitation energy through two BChls that form a strongly interacting dimer, the so-called special pair. The special pair are in close proximity to two additional BChls named accessory BChls (see Fig. 7 *c*). Interestingly, the RC BChls absorb at slightly higher energies (at 865 nm for the special pair and at 802 nm for accessory BChls) than the B875 BChls of LH-I (Woodbury and Allen,

FIGURE 8 Basic bacterial photo-synthetic unit (PSU), including the LH-I—RC complex and LH-II. The LH-I—RC complex of *Rb. sphaeroides* is modeled in this work; the LH-II is from *Rs. molischianum* as described previously (Koepke et al., 1996); bacteriochlorophyll molecules are represented as squares. Colors are the same as in Fig. 5. Produced with the program VMD (Humphrey et al., 1996).
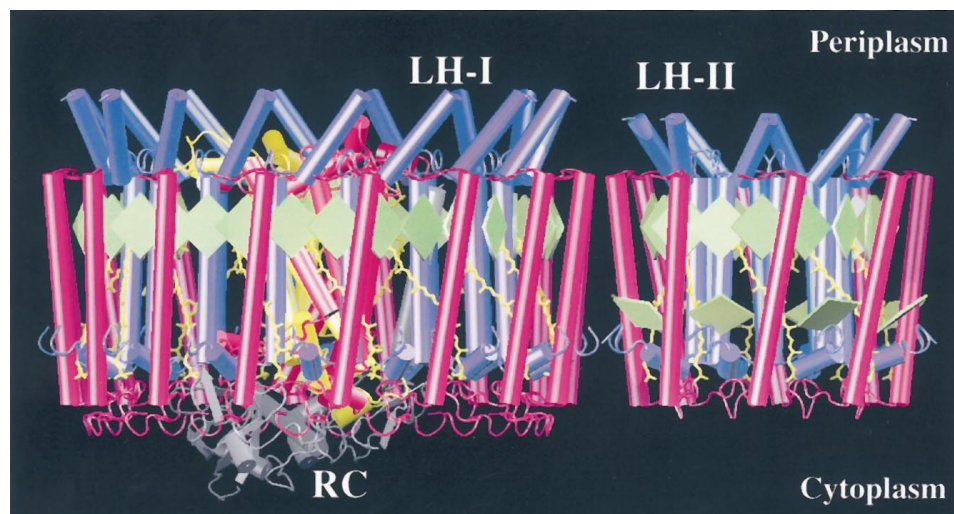
1995). Energy transfer from light-harvesting complexes II and I to the RC occurs within 100 ps and with high efficiency (near 95%) (Fleming and van Grondelle, 1994; Pullerits and Sundstrom, 1996). Knowledge of the pigment organization established here provides a basis for studies of the pathways of excitation transfer and the underlying transfer mechanisms (Hu et al., 1997; Ritz et al., 1998; Damjanović et al., 1998; Zerner et al., 1998).

The BChls in the ring-like aggregates are in close proximity; their Mg–Mg distances of 8.9–9.2 Å approach the small value (8.0 Å) of the BChls in the RC special pair (Ermler et al., 1994). The resulting strong interaction between the Q_y excited states of individual BChls is likely to overcome thermal disorder and give rise to delocalized coherent excitations, so-called excitons (Frenkel, 1931; Franck and Teller, 1938; Dracheva et al., 1996; Sauer et al., 1996). Quantum chemical calculations of the circular aggregate of 16 BChls in LH-II (Zerner et al., 1998; Hu et al., 1997; Ritz et al., 1998) revealed that the lowest-energy exciton is optically forbidden, and hence, one expects that in LH-II and, by analogy, in LH-I, the thermally relaxed excitations in the PSU conserve light energy rather than engage in fluorescence. Despite their lack of oscillator strength, the lowest-energy exciton state couples effectively to excitons of other light-harvesting complexes and to the RC bacteriochlorophylls (Hu et al., 1997). In fact, an effective Hamiltonian description for the BChl aggregates in the PSU based on the geometry of the complex shown in Fig. 8 yields close agreement with the extremely fast excitation energy transfer rates observed (Fleming and van Grondelle, 1994; Pullerits and Sundstrom, 1996; Hu et al., 1997). An important factor in this description is a co-planar alignment of the transition dipole moments of the BChl Q_y transition fixed through hydrogen bonds with the histidine side groups as described above. We note that such a co-planar arrangement of BChls was not observed in plant light-harvesting complex LHC-II (Kühlbrandt et al., 1994), nor in the recently determined 4-Å x-ray structure of photosystem I of cyanobacterium *Synechococcus elongatus* (Krauss et al., 1996).

A most interesting aspect of the pigment organization in the LH-I—RC complex shown in Fig. 7 *c* is the relative arrangement of the BChls of LH-I, of the special pair (P_A and P_B), and of the accessory bacteriochlorophylls (B_A and B_B). The latter are spatially more proximate to BChls of LH-I. This suggests that the accessory bacteriochlorophylls mediate the energy transfer from LH-I to the RC special pair. Indeed, the effective Hamiltonian approach in Hu et al., 1997, suggests that the energy transfer rate from LH-I to the special pair is enhanced by an order of magnitude through the accessory bacteriochlorophylls arranged as suggested in the present study.

The coordinates of the modeled LH-I complex and the entire bacterial PSU model can be obtained from the authors upon request.

REFERENCES

Aagaard, J., and W. Sistrom. 1972. Control of synthesis of reaction center bacteriochlorophyll in photosynthetic bacteria. *Photochem. Photobiol.* 15:209–225.

Allen, J. P., T. O. Yeates, H. Komiya, and D. C. Rees. 1987. Structure of the reaction center from *Rhodobacter sphaeroides* R-26: the protein subunits. *Proc. Natl. Acad. Sci. U.S.A.* 84:6162–6166.

Altschul, S. F., W. Gish, W. Miller, E. W. Myers, and D. J. Lipman. 1990. Basic local alignment search tool. *J. Mol. Biol.* 215:403–410.

Barz, W., A. Vermeglio, F. Francia, G. Venturoli, B. Melandri, and D. Oesterhelt. 1995. Role of the PufX protein in photosynthetic growth of *Rhodobacter sphaeroides*. II. PufX is required for efficient ubiquinone/ubiquinol exchange between the reaction center Q_B site and the cytochrome bc1 complex. *Biochemistry.* 34:15248–15258.

Boonstra, A. F., L. Germeroth, and E. J. Boekema. 1994. Structure of the light harvesting antenna from *Rhodospirillum molischianum* studied by electron microscopy. *Biochim. Biophys. Acta.* 1184:227–234.

Boonstra, A. F., R. W. Visschers, F. Calkoen, R. van Grondelle, E. F. van Bruggen, and E. J. Boekema. 1993. Structural characterization of the B800–850 and B875 light-harvesting antenna complexes from *Rhodobacter-sphaeroides* by electron microscopy. *Biochim. Biophys. Acta.* 1142:181–188.

Brooks, B. R., R. E. Bruccoleri, B. D. Olafson, D. J. States, S. Swaminathan, and M. Karplus. 1983. CHARMm: a program for macromolecular energy, minimization, and dynamics calculations. *J. Comp. Chem.* 4:187–217.

Brünger, A. T. 1996. X-PLOR, Version 3.8: A System for X-ray Crystallography and NMR. The Howard Hughes Medical Institute and Department of Molecular Biophysics and Biochemistry, Yale University, New Haven, CT.

Brunisholz, R., F. Jay, F. Suter, and H. Zuber. 1985. The light-harvesting polypeptides of *Rhodopseudomonas viridis*: the complete amino-acid sequences of B1015-α, B1015-β and B1015-γ. *Biol. Chem. Hoppe-Seyler.* 366:87–98.

CCP4. 1994. Collaborative computer project number 4, the CCP4 suite: programs for protein crystallography. *Acta Crystallogr. D.* 50:760–763.

Cowan, S. W., T. Schirmer, G. Rummel, M. Steiert, R. Ghosh, R. A. Pauptit, J. N. Jansonius, and J. P. Rosenbusch. 1992. Crystal structures explain functional properties of 2 *E. coli* porins. *Nature.* 358:727–733.

Damjanović, A., T. Ritz, and K. Schulten. 1998. Energy transfer between carotenoids and bacteriochlorophylls in a light harvesting protein. *Phys. Rev. E.* In press.

Deisenhofer, J., O. Epp, K. Miki, R. Huber, and H. Michel. 1985. Structure of the protein subunits in the photosynthetic reaction center of *Rhodopseudomonas viridis* at 3 Å resolution. *Nature.* 318:618–624.

Dracheva, T. V., V. I. Novoderezhkin, and A. Razjivin. 1996. Exciton delocalization in the antenna of purple bacteria: exciton spectrum calculations using x-ray data and experimental site inhomogeneity. *FEBS Lett.* 387:81–84.

Drews, G., and J. R. Golecki. 1995. Structure, molecular organization, and biosynthesis of membranes of purple bacteria. *In* Anoxygenic Photosynthetic Bacteria. R. E. Blankenship, M. T. Madigan, and C. E. Bauer, editors. Kluwer Academic Publishers, Dordrecht, The Netherlands. 231–257.

Engelhardt, H., A. Engel, and W. Baumeister. 1986. Stoichiometric model of the photosynthetic unit of *Ectothiorhodospira halochloris*. *Proc. Natl. Acad. Sci. U.S.A.* 83:8972–8976.

Engelman, D. M., T. A. Steitz, and A. Goldman. 1986. Identifying nonpolar transbilayer helices in amino acid sequences of membrane proteins. *Ann. Rev. Biophys. Biophys. Chem.* 15:321–353.

Engh, R. A., and R. Huber. 1991. Accurate bond and angle parameters for x-ray protein structure refinement. *Acta Crystallogr. A.* 47:392–400.

Ermler, U., G. Fritzsch, S. K. Buchanan, and H. Michel. 1994. Structure of the photosynthetic reaction center from *Rhodobacter sphaeroides* at 2.65 Å resolution: cofactors and protein-cofactor interactions. *Structure.* 2:925–936.

Farchaus, J., H. Gruenberg, and D. Oesterhelt. 1990. Complementation of a reaction center-deficient *Rhodobacter sphaeroides* pufLMX deletion strain in trans with pufBALM does not restore the photosynthesis-positive phenotype. *J. Bacteriol.* 172:977–985.

Farchaus, J., and D. Oesterhelt. 1989. A *Rhodobacter sphaeroides puf* L, M, and X deletion mutant and its complementation in trans with a 5.3 kb *puf* operon shuttle fragment. *EMBO J.* 8:47–54.

Fleming, G. R., and R. van Grondelle. 1994. The primary steps of photosynthesis. *Phys. Today* 47:48–55.

Flores, T. P., C. A. Orengo, D. S. Moss, and J. M. Thornton. 1993. Comparison of conformational characteristics in structurally similar protein pairs. *Protein Sci.* 2:1811–1826.

Franck, J., and E. Teller. 1938. Migration and photochemical action of excitation energy in crystals. *J. Chem. Phys.* 6:861–872.

Frenkel, J. 1931. On the transformation of light into heat in solids. I. *Phys. Rev.* 37:17–44.

Geourjon, C., and G. Deleage. 1994. SOPM: a self optimised prediction method for protein secondary structure prediction. *Protein Eng.* 7:157–164.

Germeroth, L., F. Lottspeich, B. Robert, and H. Michel. 1993. Unexpected similarities of the B800–850 light-harvesting complex from *Rhodospirillum molischianum* to the B870 light-harvesting complexes from other purple photosynthetic bacteria. *Biochemistry.* 32:5615–5621.

Ghosh, R., H. Hauser, and R. Bachofen. 1988. Reversible dissociation of the B873 light-harvesting complex from *Rhodospirillum rubrum* G9+. *Biochemistry.* 27:1004–1014.

Gouterman, M. 1961. Spectra of porphyrins. *J. Mol. Spectrosc.* 6:138–163.

Holley, L. H., and M. Karplus. 1991. Neural networks for protein structure prediction. *Methods Enzymol.* 202:204–224.

Hu, X., A. Damjanovic, T. Ritz, and K. Schulten. 1998. Architecture and function of the light harvesting apparatus of purple bacteria. *Proc. Natl. Acad. Sci. U.S.A.* 95:5935–5941.

Hu, X., T. Ritz, A. Damjanovic, and K. Schulten. 1997. Pigment organization and transfer of electronic excitation in the purple bacteria. *J. Phys. Chem. B.* 101:3854–3871.

Hu, X., and K. Schulten. 1997a. How nature harvests sunlight. *Phys. Today.* 50:28–34.

Hu, X., and K. Schulten. 1997b. Pigment organization of bacterial photosynthetic membrane and dynamics of energy transfer. *Biophys. J.* 72:A125.

Hu, X., D. Xu, K. Hamer, K. Schulten, J. Koepke, and H. Michel. 1995. Predicting the structure of the light-harvesting complex II of *Rhodospirillum molischianum. Protein Sci.* 4:1670–1682.

Hu, X., D. Xu, K. Hamer, K. Schulten, J. Koepke, and H. Michel. 1996. Knowledge-based structure prediction of the light-harvesting complex II of *Rhodospirillum molischianum. In* Global Minimization of Nonconvex Energy Functions: Molecular Conformation and Protein Folding. P. M. Pardalos, D. Shalloway, and G. Xue, editors. American Mathematical Society, Providence, RI. 97–122.

Humphrey, W. F., A. Dalke, and K. Schulten. 1996. VMD: Visual Molecular Dynamics. *J. Mol. Graphics.* 14:33–38.

Hunter, C. N., J. D. Pennoyer, J. N. Sturgis, D. Farrelley, and R. A. Niederman. 1988. Oligomerization states and associations of light-harvesting pigment-protein complexes of *Rhodopseudomonas sphaeroides* as analysed by lithium dodecyl sulphate-polyacrylamide gel electrophoresis. *Biochemistry.* 27:3459–3467.

Jay, F., M. Lambillotte, W. Stark, and K. Mühlethaler. 1984. The preparation and characterization of native photoreceptor units from the thylakoids of *Rhodopseudomonas viridis. EMBO J.* 3:773–776.

Joo, T., Y. Jia, J.-Y. Yu, D. Jonas, and G. Fleming. 1996. Dynamics in isolated bacterial light harvesting antenna LH2 of *Rhodobacter sphaeroides* at room temperature. *J. Phys. Chem.* 100:2399–2409.

Kabsch, W., and C. Sander. 1983. Dictionary of protein secondary structure: pattern recognition of hydrogen-bonded and geometrical features. *Biopolymers.* 22:2577–2637.

Karrasch, S., P. A. Bullough, and R. Ghosh. 1995. 8.5 Å projection map of the light-harvesting complex I from *Rhodospirillum rubrum* reveals a ring composed of 16 subunits. *EMBO J.* 14:631–638.

Kiley, P. J., T. J. Donohue, W. A. Havelka, and S. Kaplan. 1987. DNA sequence and in vitro expression of the B875 light-harvesting polypeptides of *Rhodobacter sphaeroides. J. Bacteriol.* 169:742–750.

Koepke, J., X. Hu, C. Münke, K. Schulten, and H. Michel. 1996. The crystal structure of the light harvesting complex II (B800–850) from *Rhodospirillum molischianum. Structure.* 4:581–597.

Krauss, N., W.-D. Schubert, O. Klukas, P. Fromme, H. T. Witt, and W. Saenger. 1996. Photosystem I at 4 Å resolution represents the first structural model of a joint photosynthetic reaction centre and core antenna system. *Nature Struct. Biol.* 3:965–973.

Kühlbrandt, W., D.-N. Wang, and Y. Fujiyoshi. 1994. Atomic model of plant light-harvesting complex by electron crystallography. *Nature.* 367:614–621.

Lancaster, C. R. D., U. Ermler, and H. Michel. 1995. The structure of photosynthetic reaction centers from purple bacteria as revealed by x-ray crystallography. *In* Anoxygenic Photosynthetic Bacteria. R. E. Blankenship, M. T. Madigan, and C. E. Bauer, editors. Kluwer Academic Publishers, Dordrecht, The Netherlands. 503–526.

Landolt-Marticorena, C., K. Williams, C. Deber, and R. Reithmeier. 1993. Non-random distribution of amino acids in the transmembrane segments of human type I single span membrane proteins. *J. Mol. Biol.* 229:602–608.

Lee, J., B. DeHoff, T. Donohue, R. Gumport, and S. Kaplan. 1989. Transcriptional analysis of puf operon expression in *Rhodobacter sphaeroides* 2.4.1 and an intercistronic transcription terminator mutant. *J. Biol. Chem.* 264:19354–19365.

Loach, P. A., and P. S. Parkes-Loach. 1995. Structure-function relationships in core light-harvesting complexes (LHI) as determined by characterization of the structural subunits and by reconstitution experiments. *In* Anoxygenic Photosynthetic Bacteria. R. E. Blankenship, M. T. Madigan, and C. E. Bauer, editors. Kluwer Academic Publishers, Dordrecht, The Netherlands. 437–471.

McDermott, G., S. Prince, A. Freer, A. Hawthornthwaite-Lawless, M. Papiz, R. Cogdell, and N. Isaacs. 1995. Crystal structure of an integral membrane light-harvesting complex from photosynthetic bacteria. *Nature.* 374:517–521.

McGlynn, P., C. Hunter, and M. Jones. 1994. The *Rhodobacter sphaeroides* PufX protein is not required for photosynthetic competence in the absence of a light harvesting system. *FEBS Lett.* 349:349–353.

Meckenstock, R. U., K. Krusche, R. A. Brunisholz, and H. Zuber. 1992. The light-harvesting core-complex and the B820-subunit from *Rhodopseudomonas marina*. II. Electron microscopic characterisation. *FEBS Lett.* 311:135–138.

Miller, K. 1982. Three-dimensional structure of a photosynthetic membrane. *Nature.* 300:53–55.

Monger, T., and W. Parson. 1977. Singlet-triplet fusion in *Rhodopseudomonas sphaeroides* chromatophores: a probe of the organization of the photosynthetic apparatus. *Biochim. Biophys. Acta.* 460:393–407.

MSI. 1994. QUANTA 4.0. Molecular Simulations Inc., Burlington, Mass.

Olsen, J. D., and C. N. Hunter. 1994. Protein structure modelling of the bacterial light-harvesting complex. *Photochem. Photobiol.* 60:521.

Olsen, J. D., G. D. Sockalingum, B. Robert, and C. N. Hunter. 1994. Modification of a hydrogen bond to a bacteriochlorophyll a molecule in the light-harvesting 1 antenna of *Rhodobacter sphaeroides*. *Proc. Natl. Acad. Sci. U.S.A.* 91:7124–7128.

Olsen, J., J. Sturgis, W. Westerhuis, G. Fowler, C. Hunter, and B. Robert. 1997. Site-directed modification of the ligands to the bacteriochlorophylls of the light-harvesting LH1 and LH2 complexes of *Rhodobacter sphaeroides*. *Biochemistry.* 36:12625–12632.

Papiz, M. Z., S. M. Prince, A. M. Hawthornthwaite-Lawless, G. McDermott, A. A. Freer, N. W. Isaacs, and R. J. Cogdell. 1996. A model for the photosynthetic apparatus of purple bacteria. *Trends Plant Sci.* 1:198–206.

Parson, W. W., and A. Warshel. 1995. Theoretical analysis of electron-transfer reaction. *In* Anoxygenic Photosynthetic Bacteria. R. E. Blankenship, M. T. Madigan, and C. E. Bauer, editors. Kluwer Academic Publishers, Dordrecht, The Netherlands. 559–575.

Persson, B., and P. Argos. 1994. Prediction of transmembrane segments in proteins utilising multiple sequence alignments. *J. Mol. Biol.* 237:182–192.

Pullerits, T., and V. Sundstrom. 1996. Photosynthetic light-harvesting pigment-protein complexes: toward understanding how and why. *Acc. Chem. Res.* 29:381–389.

Ritz, T., X. Hu, A. Damjanović, and K. Schulten. 1998. Excitons and excitation transfer in the photosynthetic unit of purple bacteria. *J. Luminesc.* 76–77:310–321.

Robert, B., and M. Lutz. 1985. Structure of antenna complexes of several Rhodospirillales from their resonance raman spectra. *Biochim. Biophys. Acta.* 807:10–23.

Sauer, K., R. J. Cogdell, S. M. Prince, A. Freer, N. W. Isaacs, and H. Scheer. 1996. Structure-based calculations of the optical spectra of the LH2 bacteriochlorophyll-protein complex from *Rhodopseudomonas acidophila*. *Photochem. Photobiol.* 64:564–576.

Savage, H., M. Cyrklaff, G. Montoya, W. Kuhlbrandt, and I. Sinning. 1996. Two-dimensional structure of light harvesting complex II (LHII) from the purple bacterium *Rhodovulum sulfidophilum* and comparison with LHII from *Rhodopseudomonas acidophila*. *Structure.* 4:243–252.

Schiffer, M., C. Chang, and F. J. Stevens. 1992. The functions of tryptophan residues in membrane proteins. *Protein Eng.* 5:213–214.

Schuler, G. D., S. F. Altschul, and D. J. Lipman. 1991. A workbench for multiple alignment construction and analysis. *Proteins Struct. Funct. Genet.* 9:180.

Shreve, A. P., J. K. Trautman, H. A. Frank, T. G. Owens, and A. C. Albrecht. 1991. Femtosecond energy-transfer processes in the B800–850 light-harvesting complex of *Rhodobacter sphaeroides* 2.4.1. *Biochim. Biophys. Acta.* 1058:280–288.

Stark, W., W. Kühlbrandt, I. Wildhaber, E. Wehrli, and K. Mühlethaler. 1984. The structure of the photoreceptor unit of *Rhodopseudomonas viridis*. *EMBO J.* 3:777–783.

Sturgis, J. N., J. D. Olsen, B. Robert, and C. N. Hunter. 1997. Functions of conserved tryptophan residues of the core light harvesting complex of *Rhodobacter sphaeroides*. *Biochemistry.* 36:2772–2778.

Theiler, R., F. Suter, V. Wiemken, and H. Zuber. 1984. The light-harvesting polypeptides of *Rhodopseudomonas sphaeroides* R-26.1. I. isolation, purification and sequence analyses. *Hoppe Seylers Z. Physiol. Chem.* 365:703–719.

van Grondelle, R., J. Dekker, T. Gillbro, and V. Sundstrom. 1994. Energy transfer and trapping in photosynthesis. *Biochim. Biophys. Acta.* 1187:1–65.

Walz, T., and R. Ghosh. 1997. Two-dimensional crystallization of the light-harvesting I reaction centre photounit from *Rhodospirillum rubrum*. *J. Mol. Biol.* 265:107–111.

Weiss, M. S., and G. E. Schulz. 1992. Structure of porin refined at 1.8 angstrom resolution. *J. Mol. Biol.* 227:493–509.

Woodbury, N. W., and J. Allen. 1995. The pathway, kinetics and thermodynamics of electron transfer in wild type and mutant reaction center of purple nonsulfur bacteria. *In* Anoxygenic Photosynthetic Bacteria. R. E. Blankenship, M. T. Madigan, and C. E. Bauer, editors. Kluwer Academic Publishers, Dordrecht, The Netherlands. 527–557.

Wu, H.-M., N. R. S. Reddy, and G. J. Small. 1997. Direct observation and hole burning of the lowest exciton level (B870) of the LH2 antenna complex of *Rhodopseudomonas acidophila* (strain 10050). *J. Phys. Chem. B.* 101:651.

Zerner, M. C., M. G. Cory, X. Hu, and K. Schulten. 1998. Electronic excitations in aggregate of bacteriochlorophylls. *J. Phys. Chem. B.* In press.

Zuber, H. 1985. Structure and function of light-harvesting complexes and their polypeptides. *Photochem. Photobiol.* 42:821–825.

Zuber, H., and R. A. Brunisholz. 1991. Structure and function of antenna polypeptides and chlorophyll-protein complexes: principles and variability. *In* Chlorophylls. H. Scheer, editor. CRC Press, Boca Raton, FL. 627–692.